Journal of Alloys and Compounds 503 (2010) 397–401

Contents lists available at ScienceDirect

Journal of Alloys and Compounds

journal homepage: www.elsevier.com/locate/jallcom

Influence of Pb doping on the structural, optical and electrical properties of nanocomposite Se–Te thin films

M.A. Majeed Khan[a,*], M. Wasi Khan[a,*], Mansour Alhoshan[a,1], M.S. AlSalhi[a,b], A.S. Aldwayyan[a,b], M. Zulfequar[c]

[a] King Abdullah Institute for Nanotechnology, King Saud University, Riyadh 114 51, Saudi Arabia
[b] Department of Physics and Astronomy, King Saud University, Riyadh 114 51, Saudi Arabia
[c] Department of Physics, Jamia Millia Islamia, New Delhi 110 025, India

ARTICLE INFO

Article history:
Received 4 March 2010
Received in revised form 30 April 2010
Accepted 3 May 2010
Available online 11 May 2010

Keywords:
Nanocomposite
XRD
Electrical transport
FESEM
FETEM
Band gap

ABSTRACT

Nanocomposite thin films of $Se_{0.80}Te_{0.20-x}Pb_x$ (x = 0.02, 0.06 and 0.10) were deposited on glass substrates at room temperature by thermal evaporation method. The prepared samples were characterized by X-ray diffraction (XRD), field emission scanning electron microscopy (FESEM), field emission transmission electron microscope (FETEM), optical and electrical transport measurements. The XRD patterns show the monoclinic crystal structure with average crystallite size ~30 nm. These results were correlated with the result obtained from SEM and TEM. All films reflect almost sphere-like particles with tightly bonded together and exhibit nearly equal sizes. The TEM images showed the average particle size about 27 nm whereas the average particle size for 2% Pb content sample was about 24 nm. The temperature dependence of dc conductivity has been reported in the temperature range 201–401 K. In low temperature region, we interpreted our results in terms of the Mott's law and the analysis is very consistent with the variable range hopping conduction mechanism; while in the high temperature region, it is due to the thermally activated tunneling of charge carriers in the band tails of localized states. The compositional dependence of the derived optical properties was found and discussed.

1. Introduction

During the past few years, there has been much interest in nanostructured materials due to their extraordinary physical and chemical properties. These materials offer many new opportunities to study fundamental surface processes in a controlled manner and this, in turn, leads to fabrication of new devices. The unique and fascinating properties of nanostructured materials have triggered tremendous motivation among scientists to explore the possibilities of using them in technological applications. In particular, the electronic and optical properties of nanostructured materials have been of interest because of their potential applications in the fabrication of microelectronics and optoelectronic devices [1–4].

Moreover, nanostructured materials are distinguished from conventional polycrystalline materials by the size of the structural units that compose them and they often exhibit properties that are drastically different from those of conventional materials. In many instances, this is a result of the large fraction of grain boundaries – the boundaries between the nanoparticles in bulk materials, and hence the percentage of surface atoms. The controlled synthesis of nanostructured materials is vital to the success of nanotechnology where various synthesis methods have since been introduced. They can be broadly classified into physical and chemical routes. Inert gas condensation [5], sputtering [6], thermal evaporation [7] pulse laser deposition [8] and high-energy ball milling [9–11] are among the examples of physical route, while chemical route includes dip-coating, precipitation [12], electro-deposition [13], and solvothermal routes [14]. Compared to other methods, thermal evaporation is one of the most cost-effective techniques for the fabrication of nanostructured materials. Several authors [15–17] have carried out studies on preparation and characterization of nanostructured materials by using different methods. Among the various chalcogenide materials, Se–Te based alloys are preferred because of their higher photosensitivity. Tellurium rich alloys have recently been the subject of extensive work with an emphasis on structural changes because of new technological applications particularly in the field of optical data storage [18]. We have incorporated third element as Pb in the Se–Te system, which may create compositional and configurational disorder with respect to the binary alloys.

In this article, we have reported the results of $Se_{0.80}Te_{0.20-x}Pb_x$ (x = 0.02, 0.06 and 0.10) thin films grown by thermal evapora-

* Corresponding authors.
E-mail addresses: majeed_phys@rediffmail.com (M.A.M. Khan), wasi@ksu.edu.sa (M.W. Khan).
[1] Chemical Engineering Department, King Saud University, Riyadh 11421, Saudi Arabia.

0925-8388/$ – see front matter © 2010 Elsevier B.V. All rights reserved.
doi:10.1016/j.jallcom.2010.05.016

tion method and characterize them with the X-ray diffraction (XRD), field emission scanning electron microscopy (FESEM), field emission transmission electron microscope (FETEM), optical and electrical transport properties. The aim of this study is to obtain valuable information about the structure and mechanism of the charge transport via temperature dependence of electrical conductivity.

2. Experimental

The $Se_{0.80}Te_{0.20-x}Pb_x$ ($x = 0.02$, 0.06 and 0.10) nanocomposite films were prepared by thermal evaporation technique. The films were grown on glass substrates at room temperature (305 K). In this method, 99.999% pure $Se_{0.80}Te_{0.20-x}Pb_x$ powder was thoroughly mixed by grinding them with pestle and mortar. Hence, the mixtures were made into pellets using hydraulic press with 3 MPa pressure. Only in pellet form it was possible to evaporate the material completely. During growth process, the substrate was cooled to 77 K using liquid nitrogen. The source material was kept in a molybdenum boat placed at a suitable distance from the substrate. The depositions were carried out in a high vacuum system having diffusion pump backed by rotary pump and with liquid nitrogen trap. Coatings were carried out in the pressure range of 2×10^{-6} mbar. The thickness of the films was monitored using a quartz crystal thickness monitor. For dc conductivity measurements, the samples were mounted in a specially designed metallic sample holder where a vacuum of about 10^{-3} Torr could be maintained throughout the measurements. The structural characterization was carried out by taking XRD pattern of the films at room temperature with the help of PANalytical X'Pert X-ray diffractometer equipped with a Ni filtered using Cu K_α ($\lambda = 1.54056$ Å) radiations as X-ray source. Additionally, the morphologies were observed by FESEM (JEOL, JSM-7600F) operating with a 15 kV accelerating voltage and TEM with a JEOL JEM-2100F ultra high resolution FETEM operating at 200 kV. The optical absorption of the films was measured using a double beam UV–vis spectrophotometer (Shimadzu 2550) in the wavelength range 300–900 nm at room temperature. A dc voltage of 1.5 V was applied across the sample and the resulting current was measured by a digital electrometer (Keithley, model 617). The temperature was measured by mounting a calibrated copper-constant as thermocouple near to the sample.

3. Results and discussion

3.1. Structural studies

The surface morphology of $Se_{0.80}Te_{0.20-x}Pb_x$ ($x = 0.02$, 0.06 and 0.10) thin films grown on glass substrates has been examined by field emission scanning electron microscopy (FESEM) as shown in Fig. 1(a–c). It is evident that the material exhibits almost spherical morphology and good monodispersity. Moreover, particles have well-defined spherical shape with poor inter-grain connectivity over the scanned area of the films. The structure of the nanocomposite films is uniform and monodisperse. The shell of the single nanospheres is smooth and homogeneous and only some little nanoparticles can be seen on the surface. Fig. 2(a–c) shows the field emission transmission electron microscopy (FETEM) images of the $Se_{0.80}Te_{0.20-x}Pb_x$ ($x = 0.02$, 0.06, and 0.10) samples. These images clearly exhibit spherical shape of the particles highly agglomerated with the monocrystalline particles. The average particle sizes of the aggregated nanoparticles were estimated by considering the minimum and maximum diameter of large number of particles and are given in Table 1. The insets of Fig. 1 show the X-ray diffraction patterns of $Se_{0.80}Te_{0.18}Pb_{0.02}$, $Se_{0.80}Te_{0.14}Pb_{0.06}$ and $Se_{0.8}Te_{0.10}Pb_{0.10}$ thin films, respectively. These patterns were compared with reference to JCPDS database and no extra phase of other compounds was observed within the detection limits of XRD analysis. All samples are nanocomposite in nature with a monoclinic structure. They exhibited preferential polycrystalline nature. The crystallite size of these films was calculated using the Scherrer's formula [19]

$$l = \frac{\lambda}{D \cos\theta} \quad (1)$$

where D is the full width at half maximum (FWHM) of the peaks and λ is the wavelength (~1.5414 Å) of the X-rays. The typical value of crystallite size was calculated from most intense peak at

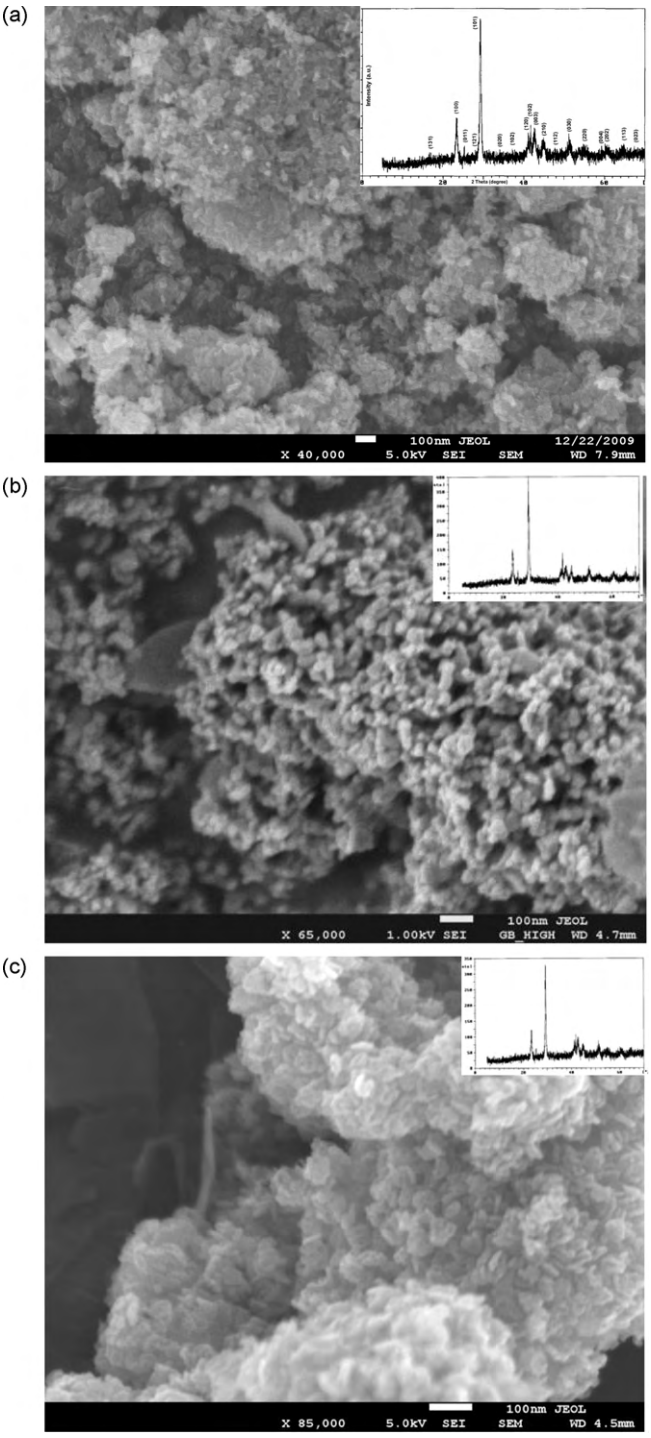

Fig. 1. FESEM micrographs of $Se_{0.80}Te_{0.20-x}Pb_x$ (a) $x = 0.02$, (b) $x = 0.06$, and (c) $x = 0.10$ thin films. The inset shows corresponding XRD pattern for the same.

$2\theta \sim 30^\circ$ for these films and tabulated in Table 1. The presence of sharp structural peaks in XRD patterns and average crystallite size of ~30 nm confirmed the nanocrystalline nature of the samples.

3.2. Optical studies

The study of materials by means of optical absorption provides simple methods for explaining some features concerning the band structure and band-gap energy. In order to obtain the fundamental

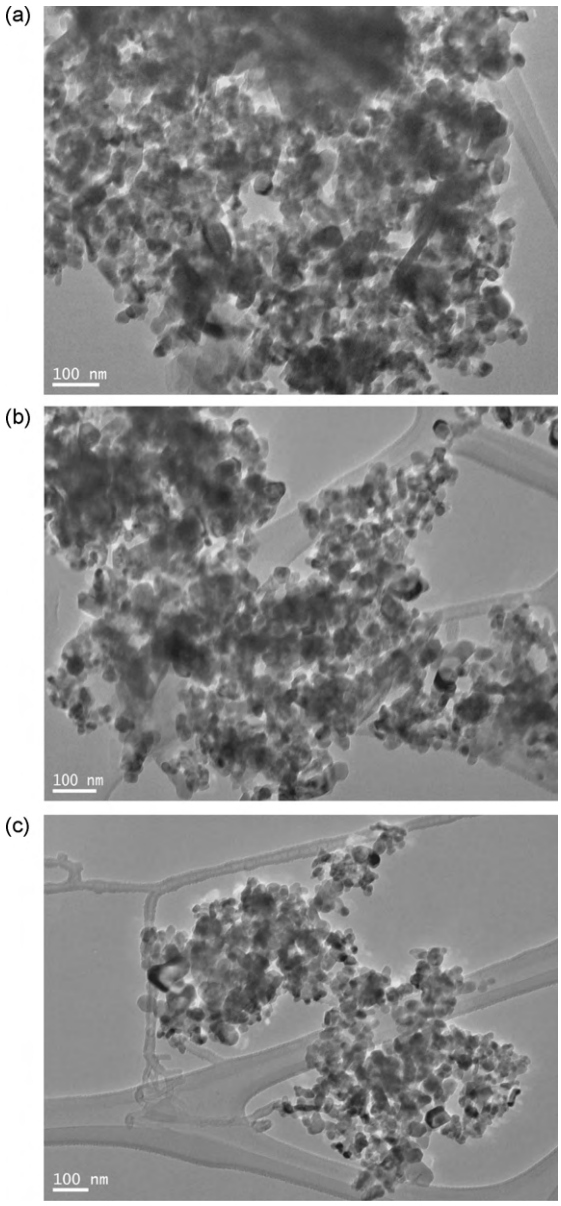

Fig. 2. FETEM images of $Se_{0.80}Te_{0.20-x}Pb_x$ (a) $x = 0.02$, (b) $x = 0.06$, and (c) $x = 0.10$ nanocomposite samples.

band-gap energy of $Se_{0.80}Te_{0.20-x}Pb_x$, we have measured the optical absorption spectra of these compositions. The absorption spectra of these compositions are studied to evaluate the absorption coefficient (α) and band-gap energy (E_g).

The absorption coefficient (α) of $Se_{0.80}Te_{0.20-x}Pb_x$ ($x = 0.02$, 0.06 and 0.10) thin films have been calculated by using well-known relation:

$$\alpha = \frac{1}{d} \ln \frac{1}{\omega} \quad (2)$$

where d is the thickness of film and ω is the absorbance.

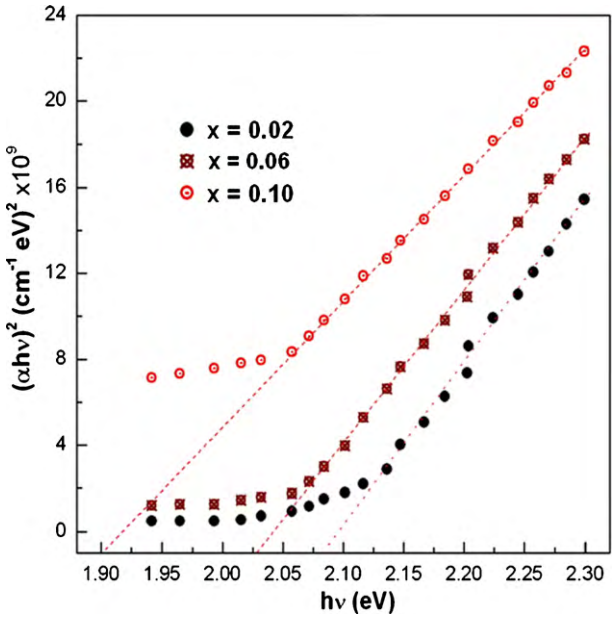

Fig. 3. UV–visible absorption spectra for $Se_{0.80}Te_{0.20-x}Pb_x$ ($x = 0.02$, 0.06 and 0.10) thin films.

The value of E_g has been determined from absorption coefficient data as a function of photon energy using the relation,

$$(\alpha h\nu) = K(h\nu - E_g)^m \quad (3)$$

where K is constant, which does not depend on photon energy and E_g is the optical band-gap energy. In the above equation $m = 1/2$ for a direct allowed transition, $m = 3/2$ for a direct forbidden transition, $m = 2$ for an indirect allowed transition and $m = 3$ for an indirect forbidden transition.

After fitting all the values of m in the above relation, the value of $m = 1/2$ is found to be hold good leading to direct transitions. Fig. 3 show the plots of $(\alpha h\nu)^2$ vs $h\nu$ for the studied thin films deposited on glass substrate at room temperature. The value of E_g for films is determined by extrapolation of the linear part of this relationship and the interception from the abscissa (at $\alpha = 0$, $E_g = h\nu$). It is clear from Fig. 3 that the direct allowed optical energy gap E_g decreased from 2.09 to 1.90 eV with the addition of Pb content. The optical band gap is strongly dependent on the fractional concentration of Pb ions. This may be due to the tendency of Pb ions to form chemical disordering and to create localized states in the band gap. According to Mott and Davis [20], the width of localized states near the mobility edge depends on the degree of disorder and defects present in the semiconducting materials. Such defects are formed due to unsaturated bonds which produce localized states in band gap. The presence of a high concentration of localized states in thin films is responsible for low optical band-gap energy. Therefore, the addition of Pb increases the concentration of localized states in the Se–Te alloy leading to the decrease in the band-gap energy. This decrease in the band-gap energy can be explained with the help of chemical bonding between the Te and Pb ions. The unsaturated bonds and an increase in particle size might be responsible for the formation of some defects, which produce

Table 1
Electrical and optical parameters of $Se_{0.80}Te_{0.20-x}Pb_x$ samples.

Sample	σ_{dc} (Ω^{-1} cm^{-1}) (336 K)	ΔE (eV) (336 K)	σ_o(Ω^{-1} cm^{-1}) (336 K)	E_g (eV)	Average particle size from TEM (nm)	Average particle size from XRD (nm)
$x = 0.02$	1.14×10^{-5}	0.44	3.83	2.09	24	27
$x = 0.06$	2.52×10^{-5}	0.35	3.80	2.03	28	30
$x = 0.10$	1.94×10^{-3}	0.29	3.71	1.90	30	33

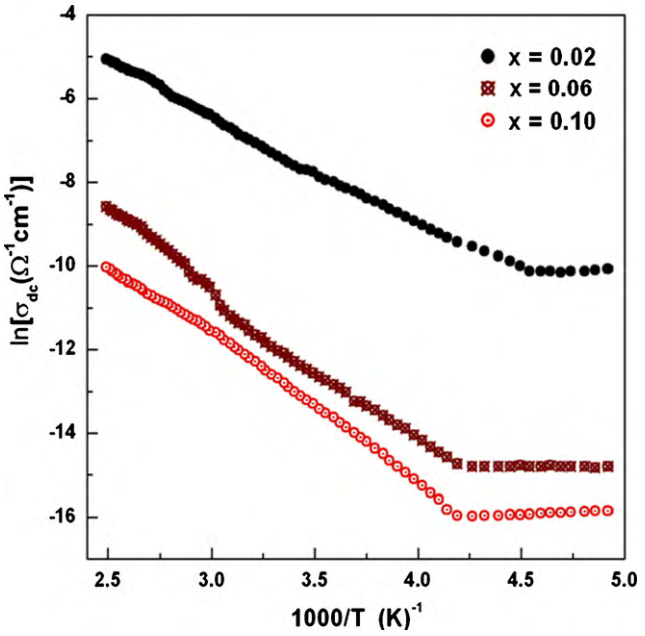

Fig. 4. Arrhenius plot of the conductivity of $Se_{0.80}Te_{0.20-x}Pb_x$ (x = 0.02, 0.06 and 0.10) thin films.

localized states in the band structure reducing the optical band gap [21].

3.3. Electrical studies

The variation of the conductivity with temperature ($\ln\sigma$ vs $10^3/T$) for $Se_{0.80}Te_{0.20-x}Pb_x$ (x = 0.02, 0.06 and 0.10) thin films are shown in Fig. 4. The electrical results exhibit two types of conduction channels which contribute two conduction mechanisms. In the high temperature region (241–401 K), the variation in $\ln\sigma$ vs $1/T$ is found to be liner indicating that the conduction in these samples is through a thermally activated process. Conductivity varies in accordance with the following relation:

$$\sigma_{dc} = \sigma_0 \exp\left(-\frac{\Delta E}{kT}\right) \tag{4}$$

where σ_0 is the pre-exponential factor, k is the Boltzmann's constant, T is the absolute temperature and ΔE is the activation energy. Table 1 shows the calculated values of the activation energy (ΔE), σ_o and the conductivity at room temperature (σ_{dc}) for various samples. One can suggest that the conduction is due to thermally assisted tunneling of charge carriers in the localized states present in the band tails. The activation energy alone cannot decide whether the conduction is occurring in the extended states or in the band tails; because these conduction mechanisms can occur simultaneously. The activation energy in the former case represents the energy difference between mobility edge and the Fermi level, $E_C - E_F$ or $E_F - E_V$; While in the later case, it represents the sum of the energy separation between the occupied localized states and the Fermi level and the mobility activation energy for the hopping process between the localized states. The pre-exponential (σ_o) factor is considered to be an important parameter in semiconductors to distinguish these two conduction processes. The value of σ_o for a-Se and Se based alloys is expected to be order of $10^4\ \Omega^{-1}\ cm^{-1}$ for conduction in the extended states [20,22]. A low value of σ_o (two or three order smaller than above value) indicates the conduction in localized states present in band tails. A still lower value of σ_o represents the conduction in localized states near the Fermi level [20,22]. In the present case, the values of σ_o are much smaller than $10^4\ \Omega^{-1}\ cm^{-1}$ (see Table 1) and hence the possibility of extended state conduction is completely ruled out and the localized state conduction in the band tails is most likely [22].

Further the incorporation of Pb ions into Se–Te results in an increase in conductivity, a decrease in activation energy and also a decrease in pre-exponential factor. These are found to be associated with the shift of the Fermi level in the impurity doped semiconductors. However, it has also been pointed out that the increase in conductivity could be caused by the increase in the portion of hopping conduction through defect states associated with the impurity atoms [22,23]. The results may be explained in terms of shift in Fermi level on the addition of Pb impurity.

At low temperature (201–240 K), for a doped semiconductor most of the free electrons are recaptured by donors itself. The electrons then have not sufficient energy to jump from donor levels to conduction band. They conduct by hopping from one level to another in the impurity band, making the free electron band conduction less important. Thus, the free electron band conduction is no more a dominating conduction mechanism in the low temperature range. In this scenario electrons hop from one donor level to the other level in the impurity band. In the hopping conduction mechanism electron jump from an occupied level to empty level, so to fulfill this condition both donor and acceptor levels are required. There are two types of hopping conduction mechanisms viz. nearest neighbor hopping (NNH) and variable range hopping (VRH), which can play significant role in conduction process of $Se_{0.80}Te_{0.20-x}Pb_x$ in the low temperature region. In the NNH conduction, electron hops to the nearest neighbor empty site. This type of conduction also needs activation energy but this activation energy has much smaller value as compared to the energy required for thermally activated band conduction. If the plot of $\ln\sigma$ with $1/T$ has two slopes one at higher and one at lower temperatures, it indicates the presence of NNH conduction. We analyzed the experimental variation of $\ln\sigma$ vs $1/T$ curve for $Se_{0.80}Te_{0.20-x}Pb_x$ films in the lower temperature region. The variations in the lower temperature region could not be fitted in a straight line suggesting that NNH type transport is not dominant in the present case. In the VRH conduction mechanism the electrons hop between the levels that are close to Fermi level irrespective of their spatial distribution. So in this type of hopping conduction the hopping distance is not constant as in NNH conduction. The VRH conduction mechanism is characterized by Mott's relation [20] as

$$\sigma = \frac{\sigma_0}{\sqrt{T}} \exp\left[\left(-\frac{T_o}{T}\right)\right]^{1/4} \tag{5}$$

The value of T_o is associated with the homogeneity and the disorder in the sample. The variable range hopping conduction process requires a value T_o/T higher than 1.where

$$\sigma_0 = 3e^2\nu\left[\frac{N(E_F)}{8\pi\alpha kT}\right]^{\frac{1}{2}} \tag{6}$$

and

$$T_0 = (\gamma\alpha^3)/(kN(E_F)) = (18\alpha^3)/(kN(E_F)) \tag{7}$$

Here $N(E_F)$, λ, α and k are the density of states at the Fermi level, a dimensionless constant, the decay constant of the wave function of the localized states near Fermi level and Boltzmann constant respectively.

Simultaneous solution of Eqs. (4) and (5) yields

$$\alpha = 22.52\sigma_0 T^{1/2}\ \ cm^{-1} \tag{8}$$

and

$$N(E_F) = 2.12 \times 10^9(\sigma_0)^3 T^{1/2}\ eV^{-1}\ cm^{-3} \tag{9}$$

Table 2
Mott parameters for $Se_{0.80}Te_{0.20-x}Pbx$ thin films in the temperature range 201–290 K.

Sample	T_o (K)	$N(E_F)$ (eV^{-1} cm^{-3})	α (cm^{-1})	R (cm)	W (meV)	αR
$x = 0.02$	4.12×10^7	7.94×10^{21}	1.21×10^8	8.32×10^{-8}	52.2	10.07
$x = 0.06$	3.03×10^7	1.74×10^{21}	6.58×10^7	1.14×10^{-7}	93.4	7.48
$x = 0.10$	1.84×10^7	7.93×10^{20}	4.28×10^7	1.46×10^{-7}	96.8	6.25

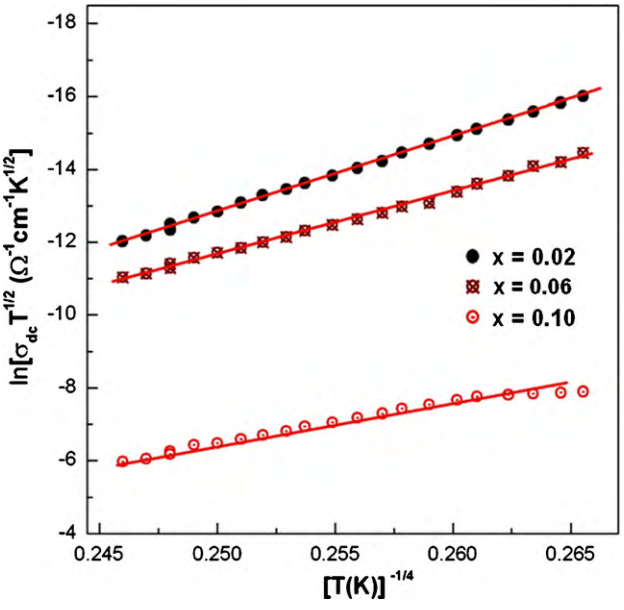

Fig. 5. $\ln \sigma T^{1/2}$ vs $T^{-1/4}$ plot for $Se_{0.80}Te_{0.20-x}Pb_x$ ($x = 0.02$, 0.06 and 0.10) thin films.

Fig. 5 shows the linear plots $\ln \sigma T^{1/2}$ vs $T^{-1/4}$ for the investigated compositions. The density of states at the Fermi levels $N(E_F)$ has been calculated for all samples and listed in Table 2. The two other hopping parameters, the average hopping distance (R) and the average hopping energy (W), according to Mott [20,24] and Hill [25] are given as

$$R = \left[\frac{9}{8\pi\alpha kTN(E_F)}\right]^{1/4} \text{cm} \quad (10)$$

and

$$W = \left[\frac{3}{4\pi R^3 N(E_F)}\right] \text{eV} \quad (11)$$

The calculated values of R and W for the samples are also listed in Table 2.

It may be quoted that when sufficient phonon energy is available; the hopping is thermally assisted and between nearest neighbors in accordance with Eq. (4). On the other hand, when the phonon energy is insufficient, the more energetic phonon assisted hops become less favourable, as a result of which the carriers will tend to hop larger distances in order to locate sites which are energetically closer than the nearest neighbors. It is difficult to distinguish between Eqs. (4) and (5), merely from the observed conductivity vs temperature variation. Only possible distinction that can be made is based on the values of αR and W. According to Mott and Davis [20,22] αR and W should have values greater than unity and kT respectively, for VRH conduction. It is evident from Table 2 that $\alpha R > 1$ and $W > kT$ and hence the present measurements are in fair agreement with the Mott condition of VRH conduction. The localized states density $N(E_F)$ decrease on incorporating the Pb element into nanocomposite Se–Te system. From above discussion, it may be concluded that at higher temperatures, conduction is taking place in the localized states of band tails; and at low temperatures, conduction is due to variable range hopping.

4. Conclusions

We have studied in detail the structural, optical and electrical properties of Pb doped Se–Te thin films by XRD, FESEM, FETEM, temperature dependent electrical conductivity and optical measurements. The XRD patterns were indexed to the monoclinic $Se_{0.80}Te_{0.20-x}Pb_x$ ($x = 0.02$, 0.06 and 0.10) structure and the average crystallite size estimated from the Scherrer's formula was between 27 and 33 nm. FETEM micrographs of the samples indicated that the films had smooth surfaces and showed that the films were nanocomposite in nature with grain size lying in the range of 24–30 nm. The optical absorption in the given system seems to be of direct type and the optical band-gap energy obtained by Tauc's extrapolation is found to decrease from 2.09 to 1.90 eV by the addition of Pb content. It is confirmed that the electrical transport of the charge carriers in nanocomposite $Se_{0.80}Te_{0.20-x}Pb_x$ thin films is governed by grain boundaries scattering processes. Hence the conductivity data in the low temperature range follow the variable range hopping mechanism. The decrease in the density of states and band-gap energy is due to increased in width of localized sates by addition of Pb from 2 to 10%. Thus we can say that Se–Te–Pb is an important material for research due to its interested optical behaviour and its potentials in many industrial applications.

Acknowledgment

The authors are grateful to the *King Abdullah Institute for Nanotechnology*, for supporting this work.

References

[1] M. Krunks, A. Katerski, T. Dedova, I. Oja Acik, A. Mere, Sol. Energy Mater. Sol. Cells 92 (2008) 1016.
[2] C. Monat, B. Alloing, C. Zinoni, L.H. Li, A. Fiore, Nano Lett. 6 (2006) 1464.
[3] B.L. Allen, P.D. Kichambare, A. Star, Adv. Mater. 19 (2007) 1439.
[4] A.L. Briseno, S.C.B. Mannsfeld, X. Lu, Y. Xiong, S.A. Jenekhe, Z. Bao, Y. Xia, Nano Lett. 7 (2007) 668.
[5] Zishan Husain Khan, M. Husain, J. Alloys Compd. 486 (2009) 774.
[6] X.B. Ning, B. Hyun, Semicond. Sci. Technol. 18 (2003) 300.
[7] D.S. Reddy, K.N. Rao, K.R. Gunasekhar, N.K. Reddy, K. Siva Kumar, P.S. Reddy, Mater. Res. Bull. 43 (2008) 3245.
[8] A. Kaushal, D. Kaur, Sol. Energy Mater. Sol. Cells 93 (2009) 193.
[9] A. Shamshad, F.A. Khan, A.S. Al-Agel, S.J. Faidah, A.A. Yaghmour, Al-Ghamdi, Mater. Lett. 64 (2010) 1391.
[10] C. Djebbari, S. Alleg, J.M. Greneche, Nucl. Instrum. Methods B 268 (2010) 306.
[11] R. Bensalem, W. Tebib, S. Alleg, J.J. Sunol, L. Bessais, J.M. Greneche, J. Alloys Compd. 471 (2009) 24.
[12] S. Jana, R. Maity, S. Das, M.K. Mitra, K.K. Chattopadhyay, Physica E 39 (2007) 109.
[13] F. Xiao, C. Hangarter, B. Yoo, Y. Rheem, K.-H. Lee, N.V. Myung, Electrochim. Acta 53 (2008) 8103.
[14] R. Seoudia, M.M. Elokr, A.A. Shabaka, A. Sobhi, Physica B 403 (2008) 152.
[15] B.Q. Cao, X.M. Teng, S.H. Heo, Y. Li, S.O. Cho, G.H. Li, W.P. Cai, J. Phys. Chem. C 111 (2007) 2470.
[16] M. Abdel Rafea, A.A.M. Farag, N. Roushdy, J. Alloys Compd. 485 (2009) 660.
[17] J. Yang, Mater. Chem. Phys. 115 (2009) 204.
[18] A. Alegria, A. Arruabarrena, F. Sanz, J. Non-Cryst. Solids 58 (1983) 17.
[19] G.W. Stewart, R.M. Morrow, Phys. Rev. 30 (1927) 232.
[20] N.F. Mott, E.A. Davis, Electronic Processes in Non-Crystalline Materials, Clarendon Press, Oxford, 1979, pp. 382.
[21] A. Zunger, J.E. Jaffe, Phys. Rev. Lett. 51 (1983) 662.
[22] N.F. Mott, E.A. Davis, Philos. Mag. 22 (1970) 903.
[23] S. Okano, M. Suzuki, K. Imura, N. Fukada, A. Hiraki, J. Non-Cryst. Solids 59/60 (1983) 969.
[24] N.F. Mott, Philos. Mag. 19 (1969) 835.
[25] R.M. Hill, Philos. Mag. 24 (1971) 1307.